JACS
JOURNAL OF THE AMERICAN CHEMICAL SOCIETY

Subscriber access provided by American Chemical Society

Article

Amphiphilic Guest Sorption of K[CrO(OOCCH)(HO)][-SiWO] Ionic Crystal

Ryosuke Kawamoto, Sayaka Uchida, and Noritaka Mizuno

J. Am. Chem. Soc., **2005**, 127 (30), 10560-10567• DOI: 10.1021/ja042333s • Publication Date (Web): 09 July 2005

Downloaded from http://pubs.acs.org on March 25, 2009

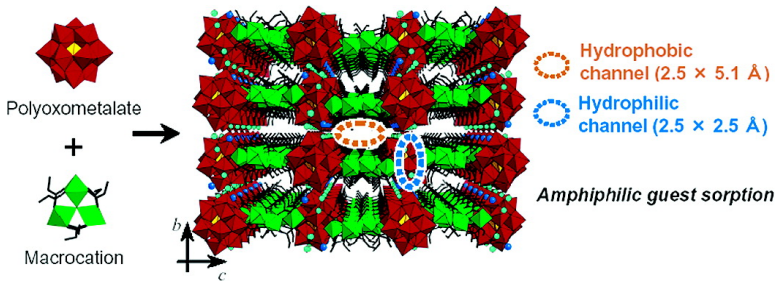

More About This Article

Additional resources and features associated with this article are available within the HTML version:

- Supporting Information
- Links to the 16 articles that cite this article, as of the time of this article download
- Access to high resolution figures
- Links to articles and content related to this article
- Copyright permission to reproduce figures and/or text from this article

View the Full Text HTML

ACS Publications
High quality. High impact.

Journal of the American Chemical Society is published by the American Chemical Society. 1155 Sixteenth Street N.W., Washington, DC 20036

J|A|C|S
ARTICLES
Published on Web 07/09/2005

Amphiphilic Guest Sorption of $K_2[Cr_3O(OOCC_2H_5)_6(H_2O)_3]_2[\alpha\text{-}SiW_{12}O_{40}]$ Ionic Crystal

Ryosuke Kawamoto, Sayaka Uchida, and Noritaka Mizuno*

Contribution from the Department of Applied Chemistry, School of Engineering, The University of Tokyo, 7-3-1 Hongo, Bunkyo-ku, Tokyo 113-8656, Japan

Received December 20, 2004; E-mail: tmizuno@mail.ecc.u-tokyo.ac.jp

Abstract: An ionic crystal $K_2[Cr_3O(OOCC_2H_5)_6(H_2O)_3]_2[\alpha\text{-}SiW_{12}O_{40}]\cdot 3H_2O$ (**1a**) is synthesized by the complexation of a Keggin-type polyoxometalate of $[\alpha\text{-}SiW_{12}O_{40}]^{4-}$ with K^+ and a macrocation of $[Cr_3O(OOCC_2H_5)_6(H_2O)_3]^+$. Compound **1a** possesses both hydrophilic and hydrophobic channels in the crystal lattice. The 3 mol mol^{-1} of the water of crystallization in **1a** resides in the hydrophilic channel. The water of crystallization is removed by the evacuation at 303 K to form the guest-free phase **1b** with small changes in the lattice lengths (±0.2 Å). The water sorption profile is reproduced by the single rate constant. Therefore, the water sorbed probably resides in the hydrophilic channel. Compound **1b** sorbs various kinds of polar organic molecules, and the amounts of $\leq C_3$ alcohols are comparable to or larger than that of water, while chlorocarbons with no hydrogen-bonding ability and nonpolar molecules are excluded. Thus, **1b** showed the amphiphilic sorption property. The states of the polar organic molecules sorbed in **1b** have been quantitatively investigated using ethanol as a probe molecule. The IR, NMR, and single-crystal X-ray diffraction studies combined with the sorption kinetics reveal that ethanol molecules are mainly sorbed into the hydrophilic channel at $P/P_0 \leq 0.5$, while the sorption into the hydrophobic channel is dominant at $P/P_0 \geq 0.6$. Thus, it is demonstrated that ethanol molecules enter both hydrophilic and hydrophobic channels of **1b**.

Introduction

The construction of micropores in crystalline solids has been studied from the viewpoints of gas storage, molecular sieve, shape-selective catalysis, and ion exchange.[1] Inorganic zeolites, for example, are composed of covalently bonded $[TO_4]$ and $[MO_6]$ units with rigid micropores, and show the shape-selective adsorption depending on the pore size.[2] The structural design of the inorganic zeolites is limited by the requirement of the $[TO_4]$ and $[MO_6]$ units. Recently, much attention has been paid toward the synthesis of metal−organic frameworks or organic zeolites constructed with organic or organometallic building blocks.[3] The structures and chemical properties such as guest sorption of the organic zeolites can be controlled by the utilization of functional groups. Some organic zeolites show the flexible structural transformation with the guest sorption by the specific host−guest interaction.[4]

Nanosized polyoxometalates, which are transition metal macroanions,[5] are suitable building blocks for novel crystalline solids[6] and can create microstructures in the crystal lattice with the combination of appropriate macrocations. Recently, we have reported the synthesis of a macrocation−polyoxometalate compound of $K_3[Cr_3O(OOCH)_6(H_2O)_3][\alpha\text{-}SiW_{12}O_{40}]\cdot 16H_2O$ with hydrophilic nanosized channels, and the shape-selective sorption of the hydrophilic guests.[7,8]

From the viewpoint of the storage and utilization of organic resources, the control of the sorption of organic guests by the crystalline solids is favorable. Because organic guests contain hydrophobic (e.g., alkyl, phenyl, etc.) and/or hydrophilic (e.g., hydroxyl, nitrile, etc.) functional groups, the construction of hydrophobic and hydrophilic spaces by the fine-tuning of the constituent elements and ligands is interesting, leading to the

(1) (a) Barton, T. J.; Bull, L. M.; Klemperer, W. G.; Loy, D. A.; McEnaney, B.; Misono, M.; Monson, P. A.; Pez, G.; Scherer, G. W.; Vartuli, J. C.; Yaghi, O. M. *Chem. Mater.* **1999**, *11*, 2633. (b) Davis, M. E. *Nature* **2002**, *417*, 813. (c) Yamamoto, K.; Sakata, Y.; Nohara, Y.; Takahashi, Y.; Tatsumi, T. *Science* **2003**, *300*, 470.

(2) (a) Csicsery, S. M. *Pure Appl. Chem.* **1986**, *58*, 841. (b) Corma, A. *Chem. Rev.* **1995**, *95*, 559. (c) van Santen, R. A.; Kramer, G. J. *Chem. Rev.* **1995**, *95*, 637. (d) Thomas, J. M. *Angew. Chem., Int. Ed.* **1999**, *38*, 3588. (e) Tsapatsis, M. *AIChE J.* **2002**, *48*, 654. (f) Serre, C.; Taulelle, F.; Férey, G. *Chem. Commun.* **2003**, 2755.

(3) Recent reviews on organic zeolites are: (a) Eddaoudi, M.; Moler, D. B.; Li, H.; Chen, B.; Reineke, T. M.; O'Keeffe, M.; Yaghi, O. M. *Acc. Chem. Res.* **2001**, *34*, 319. (b) Moulton, B.; Zaworotko, M. J. *Chem. Rev.* **2001**, *101*, 1629. (c) Kitagawa, S.; Kitaura, R.; Noro, S. *Angew. Chem., Int. Ed.* **2004**, *43*, 2334. Recent reports on organic zeolites are: (d) Fujita, M.; Kwon, Y. J.; Washizu, S.; Ogura, K. *J. Am. Chem. Soc.* **1994**, *116*, 1151. (e) Seo, J. S.; Whang, D.; Lee, H.; Jun, S. I.; Oh, J.; Jeon, Y. J.; Kim, K. *Nature* **2000**, *404*, 982. (f) Kosal, M. E.; Chou, J. H.; Wilson, S. R.; Suslick, K. S. *Nat. Mater.* **2002**, *1*, 118. (g) Kitaura, R.; Kitagawa, S.; Kubota, Y.; Kobayashi, T. C.; Kindo, K.; Mita, Y.; Matsuo, A.; Kobayashi, M.; Chang, H. C.; Ozawa, T. C.; Suzuki, M.; Sakata, M.; Takata, M. *Science* **2002**, *298*, 2358. (h) Pan, L.; Liu, H.; Lei, X.; Huang, X.; Olson, D. H.; Turro, N. J.; Li, J. *Angew. Chem., Int. Ed.* **2003**, *42*, 542. (i) Pan, L.; Adams, K. M.; Hernandez, H. E.; Wang, X.; Zheng, C.; Hattori, Y.; Kaneko, K. *J. Am. Chem. Soc.* **2003**, *125*, 3062. (j) Bradshaw, D.; Prior, T. J.; Cussen, E. J.; Claridge, J. B.; Rosseinsky, M. J. *J. Am. Chem. Soc.* **2004**, *126*, 6106.

(4) (a) Serre, C.; Millange, F.; Thouvenot, C.; Noguès, M.; Marsolier, G.; Louër, D.; Férey, G. *J. Am. Chem. Soc.* **2002**, *124*, 13519. (b) Uemura, K.; Kitagawa, S.; Fukui, K.; Saito, K. *J. Am. Chem. Soc.* **2004**, *126*, 3817.

(5) (a) Pope, M. T.; Müller, A. *Angew. Chem., Int. Ed. Engl.* **1991**, *30*, 34. (b) Okuhara, T.; Mizuno, N.; Misono, M. *Adv. Catal.* **1996**, *41*, 113. (c) Hill, C. L., Ed. Polyoxometalates. *Chem. Rev.* **1998**, *98*, 1. (d) Neumann, R. *Prog. Inorg. Chem.* **1998**, *47*, 317.

10.1021/ja042333s CCC: $30.25 **© 2005 American Chemical Society**

control of the structural arrangement and orientation of organic guests and to unique selectivity in the sorption, catalysis, etc. For example, Inagaki et al. have reported the synthesis of a mesoporous organosilica material composed of well-ordered hydrophilic and hydrophobic layers.[9] Robson et al. have reported the synthesis of a zinc saccharate material with hydrophilic and hydrophobic channels, which are isolated from each other.[10] However, the hydrophilic and hydrophobic channel properties have not yet been exploited.

Herein, we report the construction of both hydrophobic and hydrophilic channels in the crystal lattice of the polyoxometalate-based compound of $K_2[Cr_3O(OOCC_2H_5)_6(H_2O)_3]_2[\alpha\text{-}SiW_{12}O_{40}]$ and the amphiphilic guest sorption properties. The states of the molecules sorbed and the structural transformation of the compound with the guest sorption are investigated with in situ IR, NMR, single-crystal XRD, and the sorption kinetic methods.

Experimental Section

Synthesis of the Ionic Crystal. $K_2[Cr_3O(OOCC_2H_5)_6(H_2O)_3]_2[\alpha\text{-}SiW_{12}O_{40}]\cdot 3H_2O$ (**1a**) was synthesized as follows: $K_4[\alpha\text{-}SiW_{12}O_{40}]\cdot nH_2O$[11] (0.60 g, ca. 0.18 mmol) and $[Cr_3O(OOCC_2H_5)_6(H_2O)_3](NO_3)\cdot nH_2O$[12] (0.16 g, ca. 0.20 mmol) were dissolved into 10 mL of distilled water, and KCl (0.16 g, 2.14 mmol) was added. The solution was then kept at 308 K for 24 h. Green crystals of **1a** were formed in 40% yield. FT-IR (KBr): 1600(br), 1534(w), 1469(s), 1442(s), 1378(w), 1307(m), 1090(w), 1016(m), 971(s, ν_{asym}(W═O)), 922(br, ν_{asym}(Si−O)), 880(m, ν_{asym}(W−Oc−W)), 802(br, ν_{asym}(W−Oe−W)), 651(m, ν_{asym}(Cr_3−O)) cm^{-1}. Anal. Calcd for $C_{36}H_{78}Cr_6K_2O_{75}SiW_{12}$: C, 9.97; H, 1.80; Cr, 7.20; K, 1.80; Si, 0.65; W, 50.90. Found: C, 9.97; H, 1.80; Cr, 7.24; K, 1.63; Si, 0.60; W, 51.11.

The guest-free phase of **1a** (**1b**) was prepared by the evacuation at 303 K for 6 h (with regard to IR and NMR measurements) or the heat treatment in a dry N_2 flow at 353 K for 1 h (with regard to XRD and sorption kinetic measurements). It was confirmed by the TG−MS measurements that only water molecules were desorbed by the treatments. The weight loss of **1a** by the evacuation at 303 K for 6 h or by the heat treatment in a dry N_2 flow at 353 K for 1 h was 1.25%. The values well agreed with the amount (1.25%) of the three molecules of water of crystallization in **1a**. The IR spectra of **1a** after the treatments showed the bands characteristic of the macrocation and polyoxometalate, showing that the molecular structures of the constituent ions are retained in **1b**.

Characterization. Compound **1a** was dissolved in water, and the solution was spread on a Si plate followed by drying in air. The Si plate was then placed into the IR cell and was evacuated at 303 K for 6 h to form **1b**. Next, **1b** was exposed to a water or ethanol vapor at 303 K. The FT-IR spectrum was recorded with a FT-IR 460 Plus spectrometer (Jasco). Each spectrum was deconvoluted with 3140, 3290, 3470, and 3550 cm^{-1} bands as described by the Gaussian function.

Compound **1a** was placed into the glass cell and evacuated at 303 K for 6 h to form **1b**. **1b** was then exposed to the $^{13}CH_3{}^{13}CH_2OH$ vapor at 303 K, and the glass cell was sealed. The glass cell was set into a zirconia rotor and spun at a MAS rate of 5 kHz at 303 K. The solid-state MAS NMR spectrum was recorded with a CMX-300 Infinity spectrometer (Chemagnetics) operating at 7.05 T. The resonance frequency for ^{13}C was 75.57 MHz, and single pulse excitation with ^1H decoupling was applied. The NMR spectrum was deconvoluted with 17-, 21-, 58-, 63-ppm bands as described by the Gaussian function.

Compound **1a** was treated in a dry N_2 flow at 353 K for 1 h to form **1b**. **1b** was then exposed to a controlled water or ethanol vapor flow (N_2 balance). The XRD pattern was measured at 303 K with XRD-DSCII (Cu Kα radiation (50 kV-200 mA), Rigaku Corp.). The DSC curve was monitored in parallel with the powder XRD pattern. An exothermic peak was observed upon the increase in the vapor pressure. The equilibrium of the vapor sorption was confirmed by the facts that the DSC curve did not show any endothermic or exothermic peaks and that the powder XRD patterns remained unchanged. The lengths of the crystal axes for **1b** were calculated using Material Studio (Accelrys Inc.). The calculation was performed by the combination of peak profile fitting using the Pawley refinement,[13] model optimization by the simulated annealing method,[14] and final structure refinement using the Rietveld method.[15]

Compound **1a** was evacuated at 303 K for 6 h to form **1b**. The sorption isotherms were measured at 298 K with an automatic sorption apparatus Omnisorp 100CX (Coulter Corp.). The P_0 values were the saturation pressures of the liquid sorbents at 298 K and were shown in parentheses: water (3.16 kPa), methanol (16.92 kPa), ethanol (7.89 kPa), 1-propanol (2.73 kPa), 2-propanol (5.93 kPa), 1-butanol (0.86 kPa), isobutanol (1.95 kPa), 2-butanol (2.35 kPa), *tert*-butyl alcohol (5.35 kPa), acetonitrile (12.20 kPa), methyl acetate (29.28 kPa), methyl formate (86.22 kPa), formic acid (5.71 kPa), diethyl ether (64.20 kPa), dichloromethane (44.28 kPa), 1,2-dichloroethane (8.84 kPa), and 1,4-dioxane(4.90 kPa). The P_0 value for the gas sorbents (methyl ether, nitrogen monoxide, nitrogen, and methane) was 101.3 kPa.

TG-DTA measurements were performed with Thermo Plus 2 (Rigaku Corporation) using $\alpha\text{-}Al_2O_3$ as a reference under a controlled vapor flow (N_2 balance). The evolved gas was quantitatively analyzed with a GCMS-QP5050A mass spectrometer system (Shimadzu). It was confirmed that the weight increase upon the introduction of water or alcohols was equal to the amounts of sorption in the sorption isotherms.

An ionic crystal of **1a** for the single-crystal X-ray structure analysis was separated from the synthetic solution and dried under atmospheric pressure (P/P_0 = ca. 0.4). The single-crystal X-ray diffraction measurement of **1a** was performed on a Rigaku Mercury diffractometer with graphite monochromated Mo Kα radiation (λ = 0.71070 Å) and a CCD 2-D detector. The unit cell was determined from the reflections collected on the setting angles of seven frames by changing by 0.5° for each frame. Two different settings were used, and the angles were changed by 0.5° per frame. Intensity data were collected with a scan width of 0.5°. The structure analysis was performed by using the Crystalstructure[16] crystallographic software package. The structure of **1a** was solved by Patterson methods by using the DIRDIFF99 program[17] and expanded using Fourier techniques.[18] In the final cycle of the full-matrix least-squares refinement, tungsten and chromium atoms were refined

(6) (a) Hölscher, M.; Englert, U.; Zibrowius, B.; Hölderich, W. F. *Angew. Chem., Int. Ed. Engl.* **1994**, *33*, 2491. (b) Hayashi, Y.; Müller, F.; Lin, Y.; Miller, S. M.; Anderson, O. P.; Finke, R. G. *J. Am. Chem. Soc.* **1997**, *119*, 11401. (c) Hagrman, D.; Hagrman, P. J.; Zubieta, J. *Angew. Chem., Int. Ed.* **1999**, *38*, 3165. (d) Son, J. H.; Choi, H.; Kwon, Y. U. *J. Am. Chem. Soc.* **2000**, *122*, 7432. (e) Schmitt, W.; Baissa, E.; Mandel, A.; Anson, C. E.; Powell, A. K. *Angew. Chem., Int.* Ed. **2001**, *40*, 3577. (f) Zhang, H.; Duan, L.; Lan, Y.; Wang, E.; Hu, C. *Inorg. Chem.* **2003**, *42*, 8053. (g) Vasylyev, M. V.; Neumann, R. *J. Am. Chem. Soc.* **2004**, *126*, 884. (h) Ishii, Y.; Takenaka, Y.; Konishi, K. *Angew. Chem., Int. Ed.* **2004**, *43*, 2702.
(7) (a) Uchida, S.; Hashimoto, M.; Mizuno, N. *Angew. Chem., Int. Ed.* **2002**, *41*, 2814. (b) Uchida, S.; Mizuno, N. *Chem.-Eur. J.* **2003**, *9*, 5850.
(8) Uchida, S.; Mizuno, N. *J. Am. Chem. Soc.* **2004**, *126*, 1602.
(9) Inagaki, S.; Guan, S.; Ohsuna, T.; Terasaki, O. *Nature* **2002**, *416*, 304.
(10) Abrahams, B. F.; Moylan, M.; Orchard, S. D.; Robson, R. *Angew. Chem., Int. Ed.* **2003**, *42*, 1848.
(11) Tézé, A.; Hervé, G. *Inorg. Synth.* **1990**, *27*, 93.
(12) Fujihara, T.; Aonahata, J.; Kumakura, S.; Nagasawa, A.; Murakami, K.; Ito, T. *Inorg. Chem.* **1998**, *37*, 3779.
(13) Pawley, G. S. *J. Appl. Crystallogr.* **1981**, *14*, 357.
(14) Engel, G. E.; Wilke, S.; König, O.; Harris, K. D. M.; Leusen, F. J. J. *J. Appl. Crystallogr.* **1999**, *32*, 1169.
(15) Rietveld, H. M. *J. Appl. Crystallogr.* **1969**, *2*, 65.
(16) *CrystalStructure 3.6.0*, Structure solution, refinement, and reporting software; Rigaku/MSC, 2004.
(17) Beurskens, P. T.; Admiraal, G.; Beurskens, G.; Bosman, W. P.; de Gelder, R.; Israel, R.; Smits, J. M. M. *DIRDIF99*; University of Nijmegen: Nijmegen, The Netherlands, 1999.
(18) Beurskens, P. T.; Admiraal, G.; Beurskens, G.; Bosman, W. P.; de Gelder, R.; Israel, R.; Smits, J. M. M. *DIRDIF94*; University of Nijmegen: Nijmegen, The Netherlands, 1994.

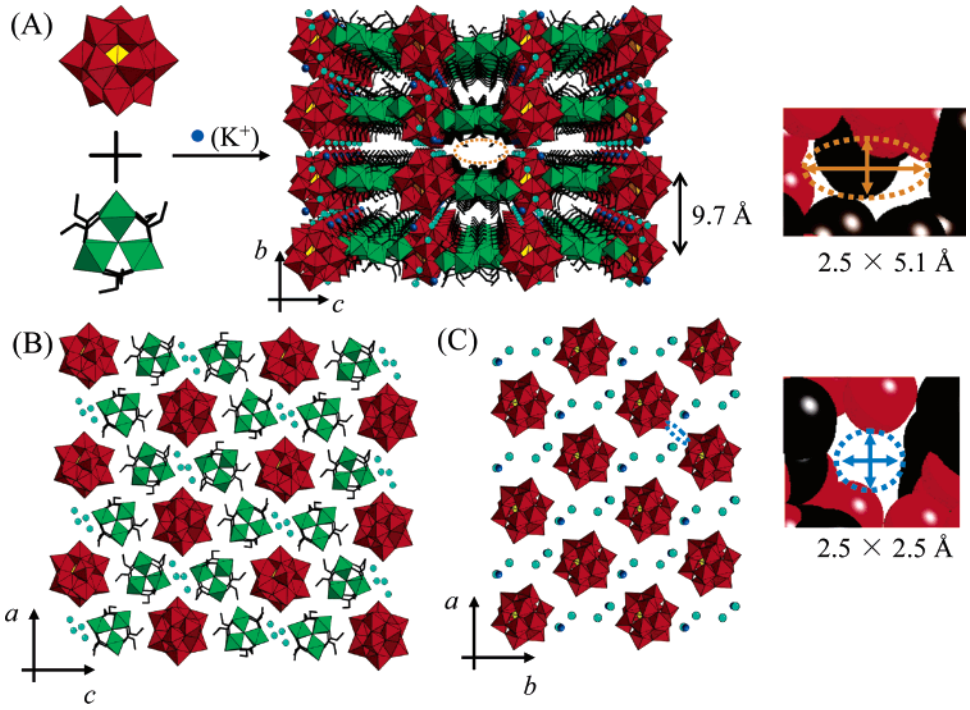

Figure 1. Synthesis and the crystal structure of **1a**. (A) Synthesis and the perspective view along the *a*-axis. Arrangements of the constituent ions and the water of crystallization in (B) *ac*-plane and (C) *ab*-plane. Red, yellow, and green polyhedra show the [WO_6], [SiO_4], and [CrO_6] units, respectively. Black lines showed the propionate ligand of the macrocation. Blue, light blue, red, and black spheres showed the potassium ion, the oxygen atoms of the water of crystallization, oxygen atom, and carbon atom, respectively. The ionic radius of potassium ion was 1.5 Å. Other atoms were drawn by their van der Waals radii (oxygen, 1.5 Å and carbon, 1.7 Å). The hydrophobic and hydrophilic channels were surrounded by the orange and blue broken lines, respectively.

Table 1. Crystallographic Data of **1a**

formula	$C_{36}O_{75}W_{12}SiCr_6K_2$
formula weight	4256.8
crystal system	monoclinic
space group	*C*2/*c*
a, Å	15.972(2)
b, Å	19.266(2)
c, Å	30.169(2)
β, deg	91.073(3)
V, Å^3	9281.6(15)
Z	4
D_c, g cm^{-3}	3.058
crystal size, mm	0.20 × 0.10 × 0.10
temperature, K	153(1)
μ(Mo, Kα), mm^{-1}	15.704
no. of measd reflections	23 716
no. of obsd reflections	8501 ($I > 3\sigma(I)$)
no. of parameters refined	329
R_1, wR_2[a]	0.059, 0.077

[a] $R_1 = \sum||F_0| - |F_c||/\sum|F_0|$; $wR_2 = [\sum w(F_0^2 - F_c^2)^2/\sum w(F_0^2)^2]^{1/2}$.

anisotropically. The other elements were refined isotropically. Neutral scattering factors were obtained from the standard source.[19]

Results

Crystal Structure of $K_2[Cr_3O(OOCC_2H_5)_6(H_2O)_3]_2[\alpha$-$SiW_{12}O_{40}]\cdot 3H_2O$ (1a). Figure 1 shows the schematic illustration of the synthesis and crystal structure of **1a**. The crystallographic data are shown in Table 1. The elemental analysis showed that the macrocation/polyoxometalate ratio in **1a** was 2:1. When the macrocation/polyoxometalate ratio in the synthetic solution was changed from 4:1 to 1:4, the stoichiometry in the complexes formed was the same as that of **1a**. The surplus anionic charge was neutralized by the potassium cations, and three molecules of the water of crystallization per formula of **1a** were found by the elemental and TG−MS analyses.

Compound **1a** was composed of layers running along the *ac*-plane, and the spacing between the layers was 9.7 Å (Figure 1A). Figure 1B shows the arrangements of the constituent ions and water of crystallization in the layer. The distances between the oxygen atoms of the polyoxometalates and macrocations, those of the adjacent macrocations, and those of the water of crystallization and macrocation were 2.6−2.7, 2.6−3.1, and 2.7 Å, respectively, and within hydrogen-bonding distances. These multiple hydrogen bondings as well as Coulomb interactions were observed in the *ac*-plane, probably stabilizing of the layer. The two potassium ions per formula were crystallographically equivalent and close to the oxygen atoms of the polyoxometalates and macrocations in the neighboring layers (K^+-O_{macro} = 2.8−2.9 Å, K^+-O_{poly} = 3.0−3.1 Å).

As indicated by the broken orange line in Figure 1A, straight channels ran along the *a*-axis between the two layers and no water of crystallization was found. The channel was surrounded by propionate ligands of the macrocations. The opening of the channel was ca. 2.5 × 5.1 Å.[20] On the other hand, winding hydrogen-bond networks of the water of crystallization existed along the [110] direction through the layers (Figure 1C). The narrowest and widest opening of the hydrophilic network channel was ca. 2.5 and 4.3 Å, respectively.[20] The 3 mol mol^{-1} of the water of crystallization in **1a** existed in two sites O1 and O2 with occupancies of 1 and 0.5, respectively, and was in the vicinity of the potassium ions (K^+-O1 = 3.1 Å, K^+-O2 = 2.5 Å). Thus, compound **1a** has both hydrophilic and hydro-

(19) *International Tables for X-ray Crystallography*; The Kynoch Press: Birmingham, England, 1974; Vol. 4.

(20) The channel openings and volumes (hydrophilic channel 20 μL g^{-1}; hydrophobic channel 23 μL g^{-1}) were estimated by using ionic radii (Cr^{3+}, K^+) and van der Waals radii (the other atoms) of the constituent elements.

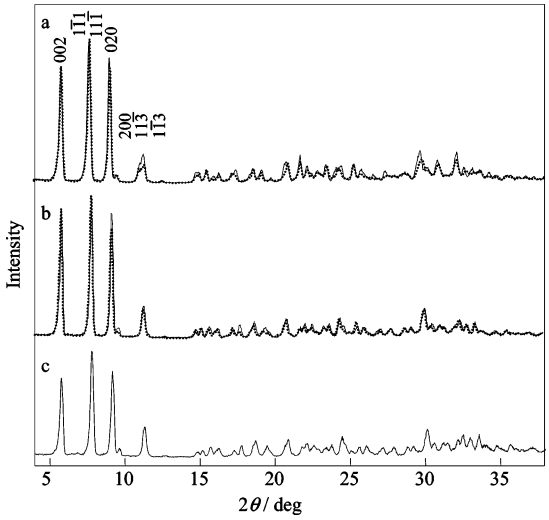

Figure 2. Powder XRD patterns of (a) **1a**, (b) **1a** under a dry N_2 flow (**1b**), and (c) **1b** after the exposure to the water vapor. The figures showed the Miller indices of each reflection ($2\theta < 15°$). (a) The calculated pattern with the single-crystal data was shown by the dotted line. (b) The calculated pattern (see Experimental Section) was shown by the dotted line.

phobic channels in the crystal lattice, which is different from the fact that $K_3[Cr_3O(OOCH)_6(H_2O)_3][\alpha\text{-}SiW_{12}O_{40}]\cdot 16H_2O$ has only the hydrophilic channel.[7] Hereafter, the straight channel surrounded by the propionate ligands of the macrocation is designated as the hydrophobic channel and the winding channel containing the water of crystallization is designated as the hydrophilic channel.

Changes in Powder XRD Patterns of 1a/1b with the Sorption−Desorption of Water. The IR spectrum of **1a** showed a broad band around 3290 cm^{-1} ($\Delta\nu_{1/2} = 300$ cm^{-1}), assignable to the ν(OH) band of the water molecules.[21] The ν(OH) band intensity for **1b** was weaker than that for **1a** and was restored by the exposure of **1b** to the saturated water vapor. Therefore, **1a** reversibly sorbs water molecules with the retention of the molecular structure of the constituent ions.

Figure 2a−c shows the powder XRD patterns of **1a**, **1b**, and **1b** after the exposure to saturated water vapor, respectively. The lengths of the crystal axes for **1a** were calculated to be $a = 16.02 \pm 0.05$ Å, $b = 19.45 \pm 0.05$ Å, and $c = 30.29 \pm 0.08$ Å. There were small changes in the peak positions with the treatment of **1a** to form **1b**. The *a* and *b* axes were shortened while the *c* axis was lengthened upon the formation of **1b**: $a = 15.85 \pm 0.07$ Å; $b = 19.25 \pm 0.08$ Å; $c = 30.41 \pm 0.15$ Å. The calculated pattern with the parameters well reproduced the observed one (dotted line in Figure 2b).[22] It follows that the volume of the unit cell decreased by 1.1×10^2 $Å^3$ from **1a** to **1b**. The positions of the diffraction peaks were restored by the exposure of **1b** to the saturated water vapor as shown in Figure 2c in accord with the IR results.

Sorption Isotherms of 1b. Figure 3 shows the sorption isotherms of **1b** at 298 K. The amount of water sorption increased with the increase in the vapor pressure and was almost leveled off (ca. 4 mol mol^{-1}) around $P/P_0 = 0.9$. Compound **1b** sorbed various kinds of polar hydrogen-bonding (hydrophilic) organic molecules such as alcohols, esters, and nitriles as well

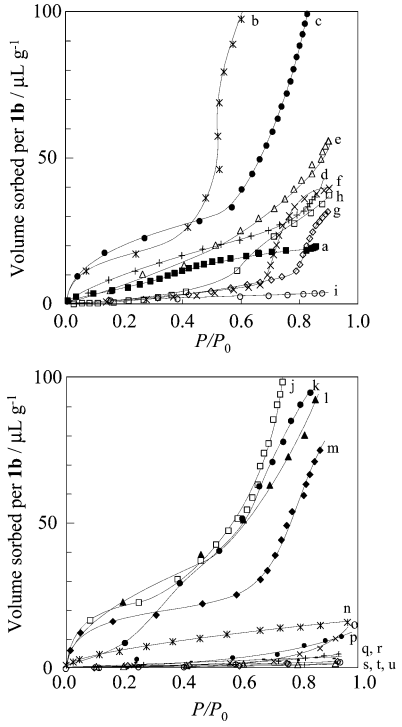

Figure 3. Sorption isotherms of **1b** at 298 K: (a) water, (b) methanol, (c) ethanol, (d) 1-propanol, (e) 2-propanol, (f) 1-butanol, (g) isobutanol, (h) 2-butanol, (i) *tert*-butyl alcohol, (j) acetonitrile, (k) methyl acetate, (l) methyl formate, (m) formic acid, (n) methyl ether, (o) ethyl ether, (p) dichloromethane, (q) 1,2-dichloroethane, (r) 1,4-dioxane, (s) nitrogen monoxide, (t) nitrogen, and (u) methane.

as water. The amounts of sorption of C_1-C_3 alcohols were larger than that of water. As for the larger C_4 alcohols, the amounts were small at $P/P_0 = 0.2$, increased suddenly at definite pressures (gate pressures), and reached 2 mol mol^{-1} around $P/P_0 = 0.9$. Neither polar non-hydrogen-bonding (hydrophobic) dichloromethane and dichloroethane nor molecules without or with small polarity such as nitrogen monoxide, dinitrogen, and methane were sorbed despite the small sizes. Figure 4 summarizes the sorption results at $P/P_0 = 0.2$. It was shown that the guest sorption properties of **1b** depended on the molecular sizes, dipole moments, and hydrogen-bonding abilities. Thus, compound **1b** showed the amphiphilic sorption property, while $K_3[Cr_3O(OOCH)_6(H_2O)_3][\alpha\text{-}SiW_{12}O_{40}]$ sorbed only water and methanol under the same conditions.[7]

Water and Ethanol Sorption Kinetics of 1b. Changes in the amount of water sorption for **1b** at $P/P_0 = 0.2$ as a function of time are shown in Figure 5. The amount gradually increased and was almost leveled off after 200 s. Similar changes were observed at $P/P_0 = 0.6$. The water sorption could be reproduced by the linear driving force mass transfer model,[23]

$$M_t = M_e\{1 - \exp(-k_1 t)\} \quad (1)$$

where M_t and M_e are the amounts of sorption at time *t* and equilibrium, respectively, and k_1 is the rate constant. $M_e = 4.7$ μL g^{-1} (1.12 mol mol^{-1}) and $k_1 = 2.8 \times 10^{-2}$ s^{-1} gave the best fit for the water sorption in Figure 5.[24]

(21) Ward, J. W. *J. Phys. Chem.* **1968**, *72*, 4211.
(22) Single-crystal X-ray structure analysis of **1b** was performed in addition to the Rietveld analysis of the powder XRD data. See ref 30 for details.
(23) (a) Foley, N. J.; Thomas, K. M.; Forshaw, P. L.; Stanton, D.; Norman, P. R. *Langmuir* **1997**, *13*, 2083. (b) Eddaudi, M.; Li, H.; Yaghi, O. M. *J. Am. Chem. Soc.* **2000**, *122*, 1391.

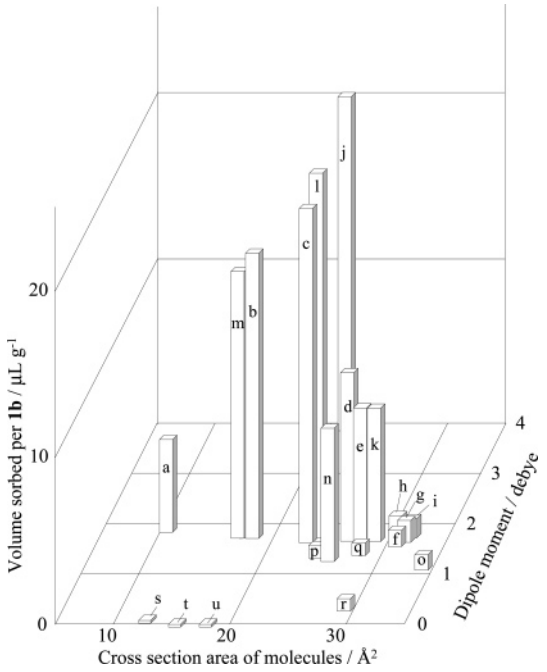

Figure 4. Effect of the cross-section areas and the dipole moments of guest molecules on the inclusion properties of **1b** at $P/P_0 = 0.2$. (a−u) Same as those in Figure 3.

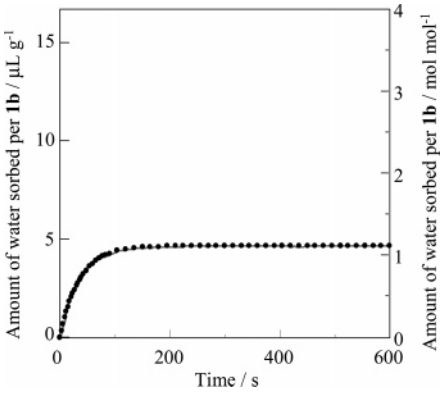

Figure 5. Changes in the amounts of water sorption for **1b** at 303 K as a function of time ($P/P_0 = 0.2$). The solid line showed the experimental data, and solid circles showed the calculated data according to eq 1.

In contrast, rapid sorption was initially observed, and then the amount gradually increased for the ethanol sorption as shown in Figure 6A and B. The sorption could not be reproduced by eq 1. Therefore, two kinds of barriers were considered according to eq 2, as in the case of the alcohol sorption for the Ni−bipyridine compound.[25]

$$M_t = M_{e1}\{1 - \exp(-k_1 t)\} + M_{e2}\{1 - \exp(-k_2 t)\} \quad (2)$$

where M_{e1} and M_{e2} are the contributions of the each of the two processes controlling the overall sorption (i.e., $M_{e1} + M_{e2} = M_e$: amounts of sorption at equilibrium), and k_1 and k_2 are the rate constants. The best fits for the ethanol sorption were given by $M_{e1} = 13.4\ \mu$L g^{-1} (0.98 mol mol^{-1}), $k_1 = 2.0 \times 10^{-3}$ s^{-1}, $M_{e2} = 4.6\ \mu$L g^{-1} (0.34 mol mol^{-1}), and $k_2 = 2.0 \times 10^{-4}$ s^{-1} at $P/P_0 = 0.2$ (Figure 6A), and $M_{e1} = 22.2\ \mu$L g^{-1} (1.63 mol

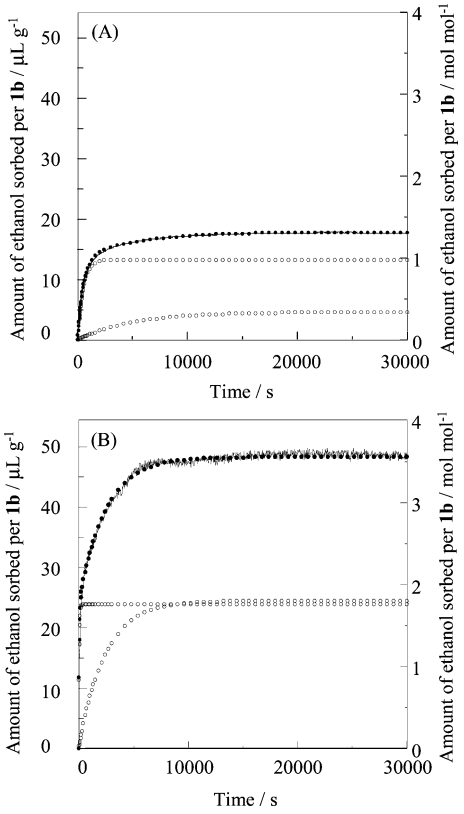

Figure 6. Changes in amounts of ethanol sorption for **1b** at 303 K as a function of time. The vapor pressures (P/P_0) are (A) 0.2 and (B) 0.6. The solid lines showed the experimental data. The solid circles showed the calculated data according to the eq 2. Open circles showed the two components for the calculation.

mol^{-1}), $k_1 = 2.2 \times 10^{-2}$ s^{-1}, $M_{e2} = 22.9\ \mu$L g^{-1} (1.68 mol mol^{-1}), and $k_2 = 4.2 \times 10^{-4}$ s^{-1} at $P/P_0 = 0.6$ (Figure 6B).

In Situ IR and ^{13}C MAS NMR Spectra of Ethanol Sorbed. Figure 7 shows the changes in the in situ IR spectra (3000−3600 cm^{-1}) of ethanol sorbed in **1b** with the ethanol vapor pressure. Liquid ethanol shows a broad ν(OH) band in the range of 3200−3500 cm^{-1} (centered around 3400 cm^{-1}).[26] A broad band appeared around 3290 cm^{-1} with a shoulder around 3470 cm^{-1} upon the introduction of the ethanol vapor ($P/P_0 = 0.05$) (Figure 7a). Both band intensities increased with increase in the ethanol vapor pressure. To quantify the ν(OH) bands, the deconvolution was carried out and the ν(OH) region was reproduced by the two main bands at 3290 and 3470 cm^{-1}. Much weaker 3140 and 3550 cm^{-1} bands were needed for the deconvolution probably because of the overlap with the strong ν(CH) band (2990 cm^{-1}) of ethanol sorbed and the strong ν-(OH) band (3650 cm^{-1}) of gaseous ethanol.

Figure 8 shows the changes in the integrated intensities of ν(OH) bands with the ethanol vapor pressure. The 3290 cm^{-1} band intensity steeply increased with the increase in the ethanol vapor pressure and did not much increase above ca. $P/P_0 = 0.4$, while the 3470 cm^{-1} band intensity gradually increased with the increase in the ethanol vapor pressure and steeply increased around $P/P_0 = 0.6$. The intensities of 3140 and 3550 cm^{-1} bands were less than 5% of the total ν(OH) band intensity. The sum of the integrated intensities of 3290 and 3470 cm^{-1}

(24) $M_e = 15.6\ \mu$L g^{-1} (3.71 mol mol^{-1}) and $k_1 = 2.3 \times 10^{-2}$ s^{-1} gave the best fit for the water sorption at $P/P_0 = 0.6$.
(25) Fletcher, A. J.; Cussen, E. J.; Bradshaw, D.; Rosseinsky, M. J.; Thomas, K. M. *J. Am. Chem. Soc.* **2004**, *126*, 9750.
(26) Yamamoto, O.; Someno, K.; Wasada, N.; Hiraishi, J.; Hayamizu, K.; Tanabe, K.; Tamura, T.; Yanagisawa, M. *Anal. Sci.* **1988**, *4*, 233.

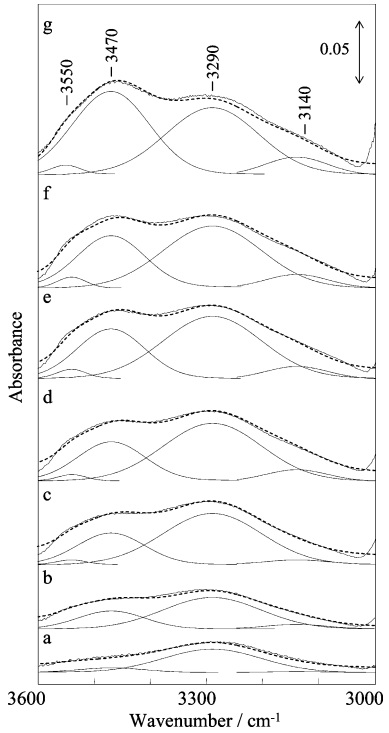

Figure 7. In situ IR spectra of ethanol sorbed in **1b** under an ethanol vapor at 303 K. P/P_0 = (a) 0.05, (b) 0.1, (c) 0.2, (d) 0.3, (e) 0.4, (f) 0.5, and (g) 0.6. The observed spectra were well reproduced by the sum (broken lines) of the deconvoluted bands (solid lines).

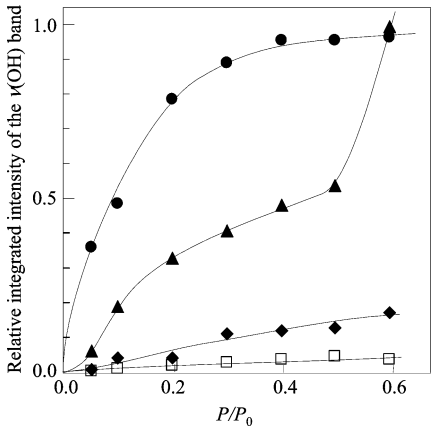

Figure 8. Changes in integrated intensities of ν(OH) band with the ethanol vapor pressure. ●, 3290 cm^{-1} band, ▲, 3470 cm^{-1} band, ◆, 3140 cm^{-1} band, and □, 3550 cm^{-1} band. The 3290 cm^{-1} band intensity at P/P_0 = 0.6 was taken as unity.

bands linearly increased with the amounts of ethanol sorption (Figure S1).

Figure 9 shows the changes in the in situ ^{13}C MAS NMR spectra of the ethanol sorbed in **1b** with the exposure to the ethanol vapor. Upon the introduction of the ethanol vapor (P/P_0 = 0.05−0.6), four signals appeared at 17, 21, 58, and 63 ppm. The low S/N ratio was due to the paramagnetic effect of Cr^{3+}.[27] Liquid ethanol (in $CDCl_3$) shows two signals at 18.1 ppm (methyl carbon) and 57.8 ppm (methylene carbon), respectively.[26] The deconvolution results were shown by the broken lines. The 17-ppm signal intensity linearly increased with

(27) The quantitative interpretation of the different NMR species is difficult because paramagnetism greatly affects the chemical shifts, intensities, and half widths of the NMR signals.[28]

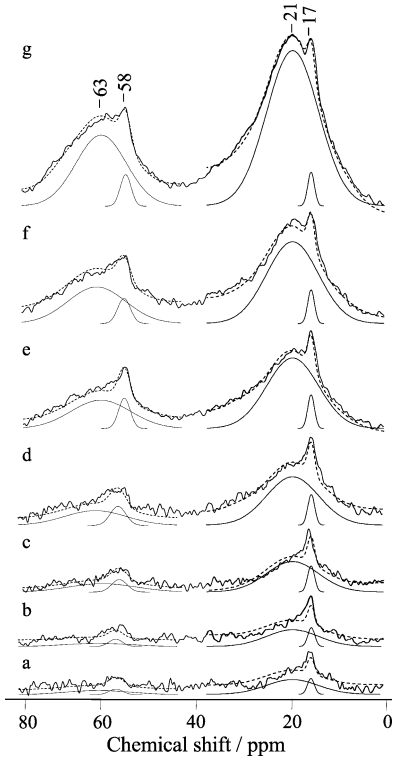

Figure 9. In situ ^{13}C MAS NMR spectrum of ethanol sorbed in **1b** under the ethanol vapor at 303 K (MAS = 5 kHz). P/P_0 = (a) 0.05, (b) 0.1, (c) 0.2, (d) 0.3, (e) 0.4, (f) 0.5, and (g) 0.6. The observed spectrum of the methyl and methylene carbon regions was approximately reproduced by the sum (broken line) of the deconvoluted bands (solid lines).

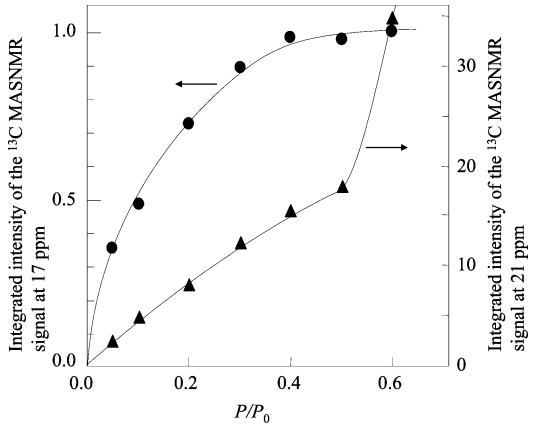

Figure 10. Changes in the integrated intensities of the methyl carbon peaks at 17 ppm (●) and 21 ppm (▲). The integrated intensity of the 17-ppm signal at P/P_0 = 0.6 was taken as unity.

the 58-ppm signal intensity in the range of P/P_0 0.05−0.6, and a similar correlation was observed between the intensities of the 21- and 63-ppm signals (Figure S2).

Figure 10 shows the changes in the integrated intensities of methyl carbon signals with the ethanol vapor pressure. The 17-ppm signal intensity steeply increased with the increase in the ethanol vapor pressure and did not much increase above P/P_0 = 0.4, while the 21-ppm signal intensity gradually increased with the increase in the ethanol vapor pressure and steeply increased around P/P_0 = 0.6. No signal was observed in the ^1H, ^{13}C (natural abundance), and ^{17}O-MAS NMR spectra of the same samples. As for the water molecules sorbed, ^1H and ^{17}O-MAS NMR spectra did not show any signals.

Discussion

Compound **1a** possessed both hydrophilic and hydrophobic channels in the crystal lattice (Figure 1). No other space where guest molecules can enter existed in the crystal lattice. The water of crystallization in **1a** was desorbed to form **1b**, and the changes in the lengths of the crystal axes were within ±0.2 Å (Figure 2). The IR spectrum of **1b** showed the characteristic bands of the macrocation and the polyoxometalate. Therefore, **1b** essentially has the same structure as **1a** and possesses the hydrophilic and hydrophobic channels in the crystal lattice.

States of Water Molecules Sorbed in 1b. Compound **1a** possessed 3 mol mol^{-1} of the water of crystallization, and the water molecules resided in the hydrophilic channel in the two positions with occupancies of 1.0 and 0.5. The water sorption isotherm of **1b** showed the amount was 4 mol mol^{-1} around $P/P_0 = 0.9$ and was almost leveled off. The water sorption profile of **1b** was reproduced by the single rate constant k_1 in the P/P_0 range 0.05−0.9. These results show that the 4 mol mol^{-1} of the water sorbed in **1b** probably resides in the hydrophilic channel and fully occupies the two sites.

States of Ethanol Molecules Sorbed in 1b. The IR spectra of the ν(OH) region mainly consisted of two bands at 3290 and 3470 cm^{-1} (Figure 7). Two ethanol species were observed by ^{13}C NMR spectroscopy (Figure 9), and there were good correlations between the intensities of the 3290 cm^{-1} ν(OH) band and the 17-ppm ^{13}C NMR signal and between the intensities of the 3470 cm^{-1} ν(OH) band and the 21-ppm ^{13}C NMR signal (Figure S3). The ethanol sorption profiles of **1b** were reproduced by the two rate constants as shown in Figure 6A and B. These results show the presence of the two kinds of ethanol molecules.

The location of the ethanol molecules sorbed in **1b** at the high relative ethanol vapor pressure ($P/P_0 = 0.5$) was investigated. (i) The amount of ethanol sorbed at $P/P_0 = 0.5$ was ca. 30 μL g^{-1} (Figure 3C). The powder XRD patterns of **1b** remained almost unchanged in the ethanol vapor pressure range of $P/P_0 = 0-0.5$ (Figure S4A), showing that **1b** sorbs the ethanol molecules without changing the crystal structure. Because the volumes of the hydrophilic and hydrophobic channels estimated from the crystal structure of **1b** were ca. 23 μL g^{-1}, respectively, the volume of ethanol sorbed at $P/P_0 = 0.5$ is larger than that of either channel. Therefore, the amount of ethanol cannot be explained by the sorption into a single channel. (ii) The coordination of methanol to the potassium ion, which was present in the hydrophilic channel of **1b**, was also observed for $K_2[Cr_3O(OOCH)_6(H_2O)_{2.5}(CH_3OH)_{0.5}]_2[\alpha\text{-}SiW_{12}O_{40}]\cdot 8CH_3OH$.[29] These results of (i) and (ii) show that at the high ethanol vapor pressure ($P/P_0 = 0.5$) the ethanol molecules are sorbed in both the hydrophilic and the hydrophobic channels.

In the powder XRD patterns of **1b** under high ethanol vapor pressure of $P/P_0 = 0.6$, new peaks attributable to the phase with expansion of 0.8 Å in the *b*-axis appeared (Figure S4B). This is probably because the total amount of ethanol sorbed was 45.1 μL g^{-1} and a little larger than the total volume (43 μL g^{-1}) of the hydrophilic and hydrophobic channels.

Next, the location of the ethanol molecules sorbed in **1b** at lower $P/P_0 = 0.2$ was investigated. (i) After the crystal of **1b** was exposed to an ethanol vapor flow ($P/P_0 = 0.2$) for 12 h (**1c**), the X-ray diffraction data were collected. Preliminary data of **1c** showed that the lattice lengths of **1b** remained almost unchanged by the sorption of ethanol and that one ethanol molecule resided in the vicinity ($K^+-O_{ethanol} = 2.9$ Å)[30] of the potassium ion, which was present in the hydrophilic channel. (ii) 1 mol mol^{-1} of ethanol observed in the hydrophilic channel of **1c** well agrees with the value of M_{e1} (0.98 mol mol^{-1}) at $P/P_0 = 0.2$ (Figure 6A) and corresponds to ca. 70% of the total ethanol molecules sorbed. The percentage well agrees with those of the 3290 cm^{-1} IR band and the 17-ppm ^{13}C NMR signal. These results of (i) and (ii) probably show that 70% of ethanol molecules (1 mol mol^{-1}) are accommodated into the hydrophilic channel at $P/P_0 = 0.2$. The assignments of IR bands and NMR signals below described further support the idea.

In general, the ν(OH) band of the alcohol molecules shifts to the lower wavenumbers with the formation of hydrogen bonding.[31] Of the two types of channels in **1b**, hydrophilic channels surrounded by the potassium ions and polyoxometalates probably possess stronger hydrogen-bonding ability. Therefore, the 3290 cm^{-1} band probably originates from ethanol molecules in the hydrophilic channels, and the 3470 cm^{-1} band originates from those in the hydrophobic channels. The chemical shifts of 17 and 58 ppm were closer to those of neat ethanol, supporting the assignment.

Conclusion

A microstructured ionic crystal $K_2[Cr_3O(OOCC_2H_5)_6(H_2O)_3]_2[\alpha\text{-}SiW_{12}O_{40}]\cdot 3H_2O$ (**1a**) was synthesized with hydrophilic and hydrophobic channels. The water of crystallization resided in the hydrophilic channel of **1a** and was removed by the evacuation at 303 K to form the guest-free phase **1b**. Compound **1b** sorbed various kinds of polar hydrogen-bonding organic molecules, and the amounts of ≤C_3 alcohols were comparable to or larger than that of water, showing amphiphilic sorption property. The polar non-hydrogen-bonding chlorocarbons and nonpolar molecules were excluded. The states of the sorbed polar organic molecules in **1b** were quantitatively investigated by in situ IR, NMR spectroscopy, the structure analysis, and the sorption kinetics using ethanol as a probe molecule. The studies showed that the ethanol molecules were mainly sorbed into the hydrophilic channel below $P/P_0 = 0.5$, while the sorption into the hydrophobic channel was dominant above $P/P_0 = 0.5$.

Acknowledgment. This work was supported in part by the Core Research for Environmental Science and Technology (CREST) program of the Japan Science and Technology Agency

(28) (a) Aime, S.; Bertini, I.; Luchinat, C. *Coord. Chem. Rev.* **1996**, *150*, 221. (b) Glass, M. M.; Belmore, K.; Vincent, J. B. *Polyhedron* **1993**, *12*, 133.

(29) The methanol molecules are in the vicinity of the potassium ion ($K^+-O_{methanol} = 2.8$ Å) and/or hydrogen bonded to the oxygen atom of the formate bridge of the macrocation ($O_{macro}-O_{methanol} = 2.4-3.0$ Å).[7]

(30) A crystal of **1a** was treated with a dry N_2 flow at 333 K to form **1b**, the crystal of **1b** was exposed to an ethanol vapor flow of $P/P_0 = 0.2$ for 12 h, and the X-ray diffraction data were collected (**1c**). The lattice lengths of **1b** ($a = 15.7371(5)$, $b = 19.1655(5)$, $c = 30.8544(11)$, $\beta = 90.7324(10)$, $V = 9305.7(5)$, $R_1 = 0.081$, w$R_2 = 0.104$) were almost the same as those of **1a** ($a = 15.972(2)$, $b = 19.266(2)$, $c = 30.169(2)$, $\beta = 91.073(3)$), as described on the basis of the Rietveld analysis of the powder XRD data. The crystal structure of **1c** was essentially the same as that of **1b**. 1 mol mol^{-1} of ethanol molecule was located in the vicinity of the potassium ion ($K^+-O_{ethanol} = 2.9$ Å), while the data were not of high quality ($R_1 = 18\%$). The oxygen atom of the ethanol molecule had the occupancy of 0.5 and was disordered between the two crystallographically equivalent potassium ions with a $K^+-O_{ethanol}$ distance of 2.9 Å.

(31) Pimentel, G. C.; McClellan, A. L. *The Hydrogen Bond*; W. H. Freeman and Co.: San Francisco and London, 1960; Chapter 3.

(JST) and Grant-in-Aid for Scientific Research from the Ministry of Education, Culture, Sports, Science, and Technology of Japan.

Supporting Information Available: Figure S1 shows the changes in the sum of integrated intensities of ν(OH) bands at 3290 and 3470 cm^{-1} with the amounts of ethanol sorption ($P/P_0 = 0.05-0.6$). Figure S2 shows the correlations between integrated intensities of 17- versus 58-ppm ^{13}C MAS NMR signals and between 21- versus 63-ppm ^{13}C MAS NMR signals. Figure S3 shows the correlation between integrated intensities of IR ν(OH) bands and ^{13}C MAS NMR signals. Figure S4 shows the changes in the in situ powder XRD patterns of **1b** at 303 K under ethanol vapor ($P/P_0 = 0-0.6$). X-ray crystallographic files of **1a** (CIF). This material is available free of charge via the Internet at http://pubs.acs.org.

JA042333S